INVESTIGATIONS OF THE WARM PRESTRESS EFFECT BY THE PRECRACKED INSTRUMENTED CHARPY TEST

H. Blumenaurer*, B. Eichler* and J. Ude*

The paper presents the potential of the precracked instrumented Charpy test to investigate the warm prestress (WPS) effect at impact loading. Experiments using an instrumented pendulum were carried out on two nuclear pressure vessel steels with different ductility. Prestressed specimens exhibit a factor of 2-3 elevation in dynamic fracture toughness relative to the values without prestressing. Causes for this enhancement are discussed in terms of residual stress measurements and fracture surface analysis.

INTRODUCTION

Warm prestressing (WPS) is a special case of over-stressing which has practical importance for the safety analysis of nuclear power plants. The term describes an apparent increase in fracture toughness in the lower shelf (cleavage fracture) after previous loading at a temperature in the ductile region. A schematic diagram of a typical WPS-cycle is shown in Fig. 1.

Several investigations have provided the WPS effect quantitatively, but experimentally evidence was only done by quasi-static fracture mechanics tests (for example (1-3)). Although the Charpy test is the most suitable test method to ensure the structural integrity of nuclear reactor pressure vessels (4), WPS results at impact loading are not available so far. For this reason the aim of this study was to analyse the WPS effect using the instrumented precracked Charpy test as a fracture mechanics approach.

* Institute of Materials Engineering and Materials Testing, Otto-von-Guericke- University Magdeburg, Germany

EXPERIMENTAL

The investigations were carried out on two nuclear pressure vessel steels (Table 1). The form-welded steel 10MnMoNi5-5 has a high ductility, and in contrast the steel 17MoV8-4 was embrittled by a special heat treatment. The microstructure of both steels was bainitic.

TABLE 1 - Chemical composition [%] and mechanical properties of the test materials

steel	C	SI	Mn	P	S	Cr	Mo	Ni	V	Al
10MnMoNi5-5	0.10	0.15	1.29	0.007	0.004	0.06	0.58	0.94	0.01	0.020
17MoV8-4	0.14	0.29	0.70	0.100	0.015	0.31	1.04	0.26	0.31	0.005

	R_c [N/mm^2]	R_m [N/mm^2]	A_5 [%]	Z [%]	KV_{max} [J]	J_{di} [N/mm]
10MnMoNi5-5	634	700	25	73	211	100 at 20°C
17MoV8-4	910 ($R_{p0.2}$)	1000	15	49	73	66 at 300°C

The specimens used were Charpy-V, fatigue precracked to a/W ≈ 0.5. Low-blow experiments were performed on an instrumented Charpy machine in accordance with the recommendations of the ESIS-TC5-Subcommittee (5). The impact velocity was about 1ms^{-1}, so that inertial effects were minimised.

The specimens of the steel 10MnMoNi5-5 were low-blow preloaded at room temperature and 300°C below the crack initiation toughness value J_{di} and afterwards broken at four temperatures in the lower shelf and transition region; the specimens of the steel 17MoV8-4 were only preloaded at 280°C and broken at 20°C. Some specimens were stress-relief annealed 550°C/2 h after preloading (LURCF).

Figure 2 illustrates a plot of force-displacement records for preloading and fracture. The J-integral of preloading at 70 and 90% of the initiation toughness J_{di} was converted into K_{WPS} values in order to enable a comparison to the fracture toughness values K_{fWPS} calculated from the well-defined maximum force.

The residual stresses at the crack tip were obtained by a computerized X-ray diffractometer; the diameter of the irradiated area was 0.2mm. The normal stress component (directions of the crack opening stress) has been measured only at one side of the ligament and mirrored to the other side. Fracture surfaces were examined by SEM to determine the stretch zone width plus ductile tearing zone ahead of the crack tip and to identify the trigger point X_c for cleavage origin (6).

RESULTS

Figure 3 shows the fracture toughness without (CF) and after (LUCF) prestressing. The WPS induced fracture toughness enhancement factor was 2 to 3 with decreasing tendency from the brittle-to-ductile transition region.

The influence of the prestress level is illustrated in Figure 4. A remarkable WPS effect can only be observed at a prestress level above 50% of the ductile initiation toughness value.

The fracture toughness values after a stress-relief heat treatment (LURCF) were lower, but they indicated that the WPS effect was not completely eliminated.

Resulting from the elastic-plastic deformation during preloading a butterfly-like compressive residual stress field with maximum values of 300 MPa was formed in a distance of 0.8 to 1.3 mm a head the crack tip (Fig5).

The SEM pictures on Figure 6 show, that after prestressing the cleavage fracture is preceded by a highly deformed stretch zone and ductile tearing with flat dimples. The stretch zone width (SZW) and the ductile tearing seam increase with temperature. Furthermore, the location of the cleavage initiation sites (Fig. 7) in the ligament was pushed away from the crack tip (Fig. 8). This observation is consistent with the weakest-link model for cleavage fracture initiation, which takes into account the competition between the nucleation of unstable microcracks and ductile tearing mechanisms. After blunting out of critical particles during preloading the crack will grow by ductile tearing until it reaches a microstructural feature (carbide) that is capable of triggering cleavage, and this dictates a higher cleavage stress. Furthermore the interaction of the compressive residual stress field due to prestressing with the crack tip process zone at reloading affects the crack driving force to propagate the cleavage crack.

CONCLUSION

The results demonstrate that the WPS effect also occurs at impact loading. The mechanisms of this effect may be explained in terms of changes of the stress distribution in the process zone due to compressive residual stresses and the weakest-link mechanism at the deformed crack tip. From this study it can be concluded, that the instrumented Charpy test using precracked specimens can be used as screening test to provide more data for scientific evaluation of the WPS effect including the influence of irradiation.

ACKNOWLEDGEMENT

The study was supported by the Bundesministerium für Bildung, Wissenschaft, Forschung und Technologie.

REFERENCES

(1) Stonesifer, R.B., Rybicki, E.F. and McCabe, D. E., Warm prestress modelling: Comparison of models and experimental results NUREG/CR-5208, MEA-2305, April 1989.
(2) Beremin, F.M. Numerical modelling of warm prestress effect using a damage function for cleavage fracture in: Advances in fracture mechanics (ECF5), Cannes, 1981, Vol. 2, 825-832.
(3) Reed P.A.A. and Knott J. Investigation of the role of residual stresses in the warm prestress (WPS) effect, Part I and II, Fatigue Fract.Engng.Mater.Struct., Vol 19, No 4, 485-513, 1996.
(4) van Walle, E. (ed). Evaluation material properties by dynamic testing, ESIS Publication 20, Mechanical Engineering Publications Ltd., London, 1996.
(5) Proposed standard methods for instrumented pre-cracked Charpy impact testing of steels, ESIS-TC5 Subcommittee, Draft 8: October 1997.
(6) Iwadate, T. and Yokobori T., Evaluation of elastic-plastic fracture toughness testing in the transition region through Japan interlaboratory tests. in: ASTM STP 1207, Philadelphia, 1994, 233-263.

Figure 1 Schematic diagram of the WPS effect

LUCF	load-unload-cool-fracture
CF	cool-fracture (non prestressed)
T_{WPS}	temperature at prestressing
T_f	temperature at fracture
K_{WPS}	stress intensity factor at prestressing
K_{fWPS}	stress intensity factor at fracture after prestressing
K_{fNWPS}	stress intensity factor at fracture without prestressing
K_{Id}	dynamic fracture toughness
J_{di}	dynamic crack initiation toughness

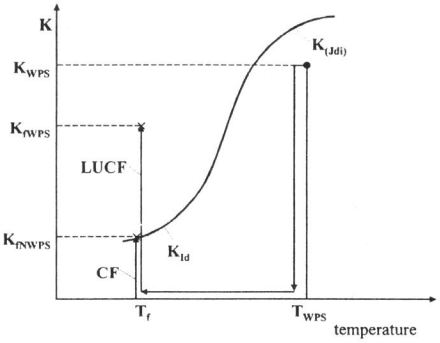

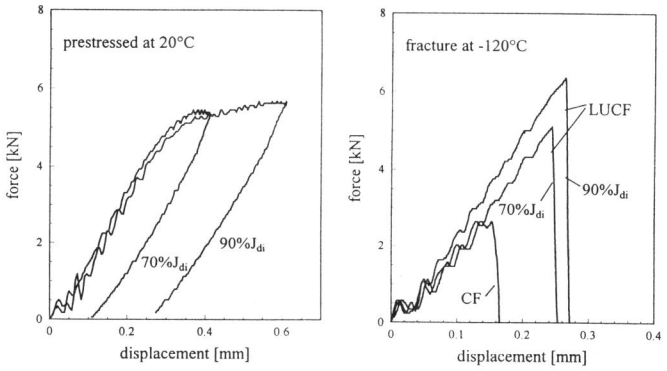

Figure 2 Force-displacement records of the steel 10MnMoNi5-5

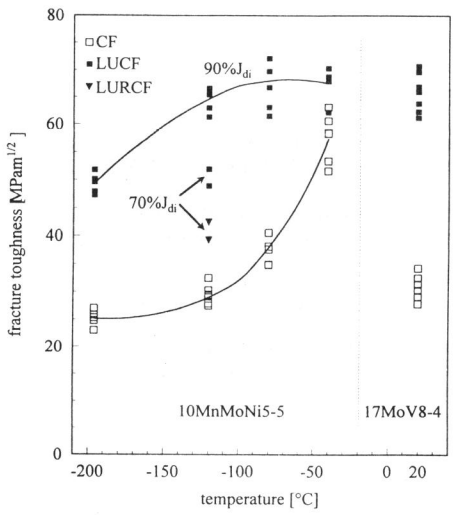

Figure 3
Fracture toughness without and after prestressing in the brittle-to-ductile transition region

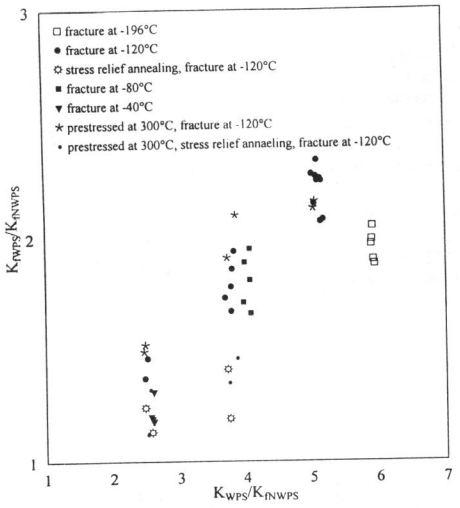

Figure 4 Enhancement of fracture toughness depending from the prestress level

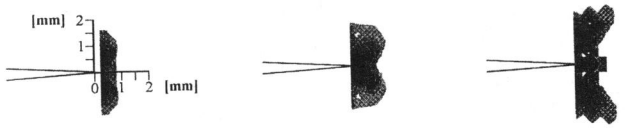

a) b) c)

Figure 5 Contour maps of the compressive residual stress field in front of the crack tip at the preloading levels a) 40 % J_{di} ; b) 90 % J_{di} ; c) 140 % J_{di} (Δa = 0.2 mm)

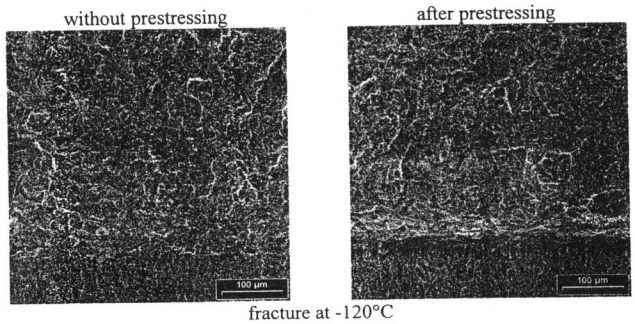

Figure 6 Fracture surfaces of the steel 10MnMoNi5-5 without and after prestressing

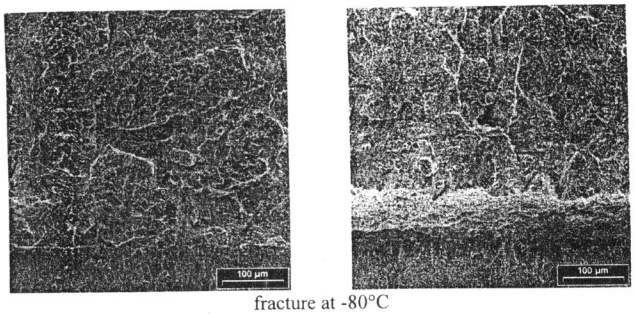

Figure 6 Fracture surfaces of the steel 10MnMoNi5-5 without and after prestressing

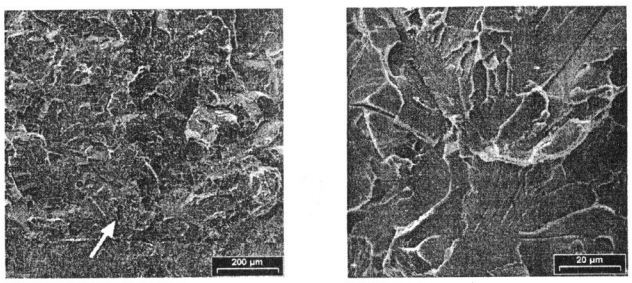

Figure 7 Clevage initiation sites of the steel 17MoV8-4

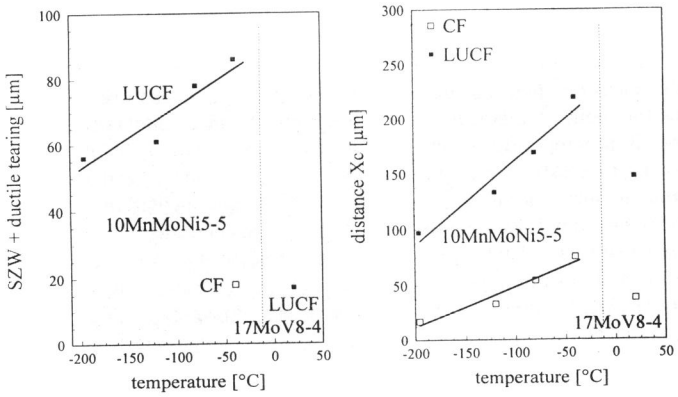

Figure 8 Influence of prestressing and temperature on ductile tearing including SZW and crack initiation point distance X_C